Journal of Metals, Materials and Minerals, Vol. 33, No. 1, pp. 47-55, 2023

Synthesis of zircon pigments from rice husk ash and their performance in ceramic glaze

Niti YONGVANICH[1,*], Peerapat SOYSOM[1], and Worachet RATKASEMSAK[1]

[1] *Department of Materials Science and Engineering, Faculty of Engineering and Industrial Technology, Silpakorn University, Nakornpathom, 73000, Thailand.*

***Corresponding author e-mail:** niti.yongvanich@gmail.com

Received date:
3 October 2022
Revised date
12 December 2022
Accepted date:
25 December 2022

Keywords:
Zircon;
Pigment;
Rice husk ash;
Industrial waste management;
Stability

Abstract

$ZrSiO_4$-based pigments have been known to be very stable in ceramic glazes but require a high firing temperature required for phase formation. This study examined the feasibility of using rice husk waste as a substitute for crystalline SiO_2. The amorphous form of silica with some impurities was obtained by calcining the rice husk at 800°C. The general chemical formula were $(Zr_{0.9}M_{0.1})SiO_4$, where M = V, Pr, Fe and Cr. The solid-state processing was achieved by firing at 1300°C for 12 h with NaF (5 wt%). X-ray Diffraction revealed a lower relative fraction between ZrO_2 (secondary phase) and $ZrSiO_4$ in the RHA systems compared to the oxide system for all dopants. Amorphousness of RHA did help enhance phase formability. The particle sizes were in the 3 µm to 5 µm range. Elemental analysis revealed some areas with intense signals of zirconium, indicating unreacted ZrO_2 particles. Colorations appeared to be blue, yellow, brown and green for dopants of V, Pr, Fe and Cr, respectively. Technological performance was tested in a practical ceramic glaze and frequently used raw materials fired at its maturation point. The results of this study hold huge potential for using rice husks for sustainable manufacturing of pigments as green products.

1. Introduction

Inorganic pigments are used in ceramic glazes to predominantly produce coloration. Several phases of pigments have been commercially employed with limitations mostly on the glaze chemistry and firing temperature. For example, malayaite-based pigments are well perceived being unstable in glazes with a high amount of ZnO. Changes in glaze's color relative to that of the pigment seem to be a major burden for ceramists for many situations. Pigments with predictable coloration after glaze maturation would be highly preferred for a wide range of glaze recipes.

Zircon-based pigments have been widely known to be thermally and chemically stable in various matured glazes [1,2]. This zirconium silicate ($ZrSiO_4$) is part of the neosilicate group with a tetragonal crystal system [3]. Its structure is composed of alternating edge-sharing ZrO_8 triangular dodecahedra and SiO_4 tetrahedra forming a chain which is joined by another chain by edge-sharing dodecahedra. Its very high melting point allows it to be employed as an opacifier in ceramic glazes. Zircon's ability to host chromophore cations also allows its use as decorative pigment with different colors such as blue, green, red-brown and yellow when doped with vanadium (V), chromium (Cr), iron (Fe) and praseodymium (Pr), respectively [1,4-7]. However, due to its dense structure with high bonding strength, incorporating those chromophore cations tends to be thermodynamically difficult with extremely high processing temperature usually required, making its production laborious and costly. The firing temperature of up to 1400°C in the solid-state processing has been frequently reported [8].

Such high firing temperature requires high energy and other laborious processing equipment. Recently, many studies have been focused on reducing the processing temperature by several methods. Wet chemical processing such as sol-gel offers advantages for utilizing lower temperatures for phase formation in addition to a higher degree of chemical homogeneity compared to its solid-state processing counterpart. However, the costs of starting precursors would have made this method less commercially feasible when producing in a large scale. Fluxes or mineralizers such as NaF and NaCl were also employed by several studies to tackle this difficulty in zircon phase formation [4,9-13]. There were still some concerns about toxicity of the by-products released during the reaction. Nevertheless, fluxing agents seemed to be commonly adopted as a solution to facilitate phase formation of zircon as well as incorporation of chromophore ions into its lattice structure. Another consideration has been toward the type of starting precursor itself. Silica can be in several forms such as crystalline quartz, fumed silica or precipitated silica. When the particle size of silica is very small (< 100 nm), it was frequently regarded as amorphous silica with a belief that its high specific surface area would be beneficial to the reactivity between highly refractory ZrO_2 and SiO_2. Another form of silica source is from rice husk ash (RHA) within which the silica content could be as high as 90% depending on its geographical areas. Extraction of pure SiO_2 from RHA using alkali and acidic treatment is a laborious and costly process and could have made this alternative source not being advantages to other sources [14]. Several studies on zircon pigment synthesis used RHA without chemical extraction but the chromophores were still limited to vanadium and praseodymium [2,15,16].

In this study, as-received RHA was used as a source of silica. Other oxide impurities in RHA would likely have minimal effect on coloration as their quantity would be very small. Other precursors were typical crystalline oxide compounds with addition of NaF in the amount of 5 wt% to help enhance reactivity in zircon phase formation. All four major colors (blue, yellow, pinkish brown and green) from V_2O_5, Pr_6O_{11}, Fe_2O_3 and Cr_2O_3 were included in this study to make it as complete as possible. The obtained pigments were also tested in a typical feldsparthic glaze to demonstrate their performance at cone 5 to 6. In addition, chemical stability of the pigments with each common glaze ingredient was examined. The results of this stability test would be useful for further development of appropriate glaze recipe for these zircon pigments.

2. Experimental

The pigments were synthesized by solid-state processing. Reagent-grade chemicals were employed except the rice husk obtained from a local rice mill. The general formula was $(Zr_{0.9}M_{0.1})SiO_4$ where M is a chromophore cation. Cr_2O_3, Fe_2O_3, Pr_6O_{11} and V_2O_5 were used as oxides supplying the four chromophore cations. Rice husks were washed with distilled water, dried at 120°C for 24 h and fired at 800°C for 2 h. This temperature was selected based on the thermo-gravimetric results. The obtained rich husk ash (RHA) was white in color and used as a source of silica (SiO_2) without taking into account of minor oxide impurities. All chemicals except NaF were dried at 300°C for 24 h and were weighed according to the previously mentioned general formula. NaF was added in the amount of 5 wt% as a flux. The mixtures were hand-ground in an agate mortar with acetone as a medium and were fired at 1300°C for 12 h with one intermediate grinding (firing for 6 h, hand-grinding and firing for another 6 h). The fired pigment samples were hand-ground again and were stored in airtight containers with silica gel. To test the technological performance, the pigments were mixed with a typical feldsparthic glaze (Na-Si-Al-Ca-Zn) in the amount of 10 wt%. The mixtures were coated on porcelain bisques and fired at 1200°C for 2 h to reach maturation in an electric furnace. For the stability test, the pigments and tested materials (glaze and raw materials) were weighed in the 1:1 ratio, hand-ground with acetone in an agate mortar and fired at 1200°C for 2 h. This firing condition would mimic that of the glaze melting.

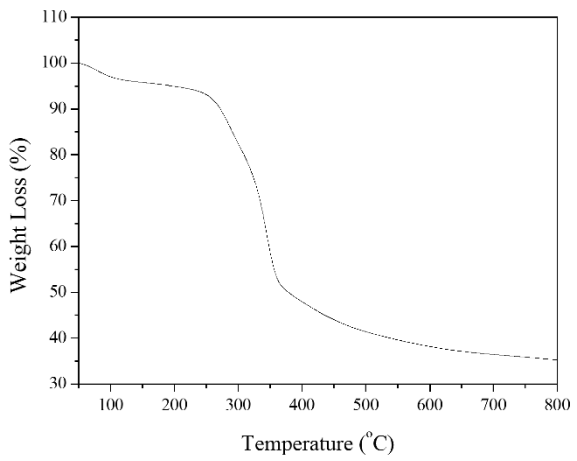

Figure 1. TGA profile of rice husk measured on heating from 50°C to 800°C in air.

Complete decomposition of organics in rice husk was determined by thermogravimetric analysis (TGA, Mettler) in air atmosphere to mimic the actual environment of the pigment synthesis. Phase formation of both RHA and pigments was examined by X-ray Diffraction (XRD, Shimadzu, 6100) in a 2-theta range of 10º to 70º (0.02º step) with 20 mA and 30 V. No crystallite size was calculated as the obtained particles exceeded the limit dictated by Warren broadening. The cell volume was calculated by lattice refinement using tungsten (W) as an internal standard. The morphology of the fired powders was investigated by Field-Emission Scanning Electron Microscopy (FeSEM, Tescan; Mira3). UV-vis-NIR spectroscopy (Shimadzu, UV-3600i) and colorimetry (X-rite, QM2000) were employed to probe the optical properties of the synthesized pigments.

3. Results and discussion

Decomposition of organics in rice husk was found by Thermo-gravimetric Analysis (TGA) to be complete at 800°C. Weight losses could be observed with three distinct steps. The first step was in the 120°C range which could be attributed by removal of hydrated species. A steep drop in weight of more than 40% occurred between 250°C and 370°C likely associated with decomposition of various organics such as cellulose and lignin-related compounds. Weight reduction continued to proceed until constancy was relatively achieved at 700°C to 800°C; this final range might be caused by other thermally stable compounds such as carbonates or chemically-bound hydrates. Therefore, the rice husks were fired at 800°C for 2 h in an electric furnace. The obtained ashes were white and brittle. They were confirmed by X-ray Diffraction to be relatively amorphous. Attempts were made to fire at higher temperatures and longer times which resulted in emergence of crystalline XRD peaks. The rice husk ash (RHA) had a particle size in the 50 nm range with isotropic shape as previously reported [14].

Phase formation of zircon pigments (RHA and oxide routes) was probed by X-ray Diffraction. The XRD patterns of the pigments fired at 1300°C for 12 h are displayed in Figure 2 and Figure 3. The undoped sample was also included for comparison. All pigment samples demonstrated major peaks of $ZrSiO_4$ (Zircon, JCPDS 06-0266) with monoclinic ZrO_2 (m-ZrO_2, JCPDS 37-1484) as a secondary phase. Longer firing times of more than 12 h did not significantly improve phase formability. Although the degree of crystallinity could not be obtained from X-ray Diffraction, utilizing the tallest peaks of all occurring phases could be used as a qualitative guide to indirectly compare the amounts of each phase [2]. The area under the peak (integrated intensity) was obtained by fitting the peak with Lorentzian function. In this case, the tallest peaks of zircon and zirconia are in the 26º and 27º range, respectively. The weight fractions of unreacted ZrO_2 and reacted $ZrSiO_4$ have been reported by using a relatively similar method of calculation including the linear absorption coefficients [11] and the peak area of tetragonal ZrO_2 [2]. However, the impurity in our study was monoclinic ZrO_2 instead of tetragonal ZrO_2. Therefore, the XRD peaks of m-ZrO_2 were used in the calculation. Given the purpose of quantitative comparison among the four dopants, this study opted to use a simpler calculation with one peak of each phase only. When comparing the highest peaks of the two phases, a noticeable decrease in the ratio of the integrated intensity between ZrO_2 and $ZrSiO_4$ was observed as shown in Table 1: Undoping (0.73),

V-doping (0.85), Pr-doping (0.80), Fe-doping (0.71) and Cr-doping (0.65). These results could likely be attributed to the refractory nature of each dopant when combined with all starting precursors, which could be beneficial toward facilitating phase formation via fluxing. The fractions of zircon from the oxide route revealed smaller values compared to those from the RHA route, except for V-doping. These results suggested that RHA, with its amorphousness, holds high potential for good reactivity during zircon phase formation.

Formation of single-phase V-doped zircon samples were rarely reported in the literature even from the gel-based processing which is known to yield better chemical homogeneity than the solid-state processing. Monoclinic ZrO_2 seemed to be the most common impurity despite the fact that the gels were fired at as high in the 1200°C to 1400°C range [1,9]. Cristobalite SiO_2 was also stated as an impurity in the pigment fired as high as 1400°C and holding time of 30 h in the study by Torres *et al.* [17]. However, in the current study (Figure 1), no SiO_2-related phases emerged, suggesting no phase transformation of the initial amorphous silica into a crystalline state during reactions with ZrO_2 and V_2O_5. A careful, slow scan did not reveal an amorphous halo as observed in an amorphous silicate glass (data not shown). Investigations using RHA with NaF as a flux by other researchers did not demonstrate this cristobalite peak but displayed only monoclinic ZrO_2 as a secondary phase when fired at or above 1000°C [15,16]. Pyon *et al*. [15] showed that $NaVO_3$ formed first as an intermediate phase with the reaction between SiO_2 and m-ZrO_2 starting at 700°C. They claimed that the Hedvall effect with enhanced reactivity during phase transitions was responsible for maximization of the reaction rate toward zircon formation. Successful doping can be verified by changes in the cell volume given the ionic radius of V^{4+}(IV) is larger than that of Si^{4+}(IV). Lattice refinement of our V-doped zircon sample yielded a cell volume of 261.50 $Å^3$ which is comparable to that reported by Ardizzone *et al.* [19]. The undoped $ZrSiO_4$ had the cell volume of 260.50 $Å^3$. Such enlargement in cell volume is testimonial to successful incorporation of vanadium ions into the tetrahedral lattice of zircon. The evidence of V cation dissolving in the $ZrSiO_4$ lattice was also confirmed by Electron Spin Resonance Spectroscopy (ESR) by Torres *et al.* whose semi-quantitative determination of such solubility was in agreement with previously reported variation in lattice parameter [17]. Whether or not a solid solubility limit was reached or achieved is beyond the scope of this study.

It is likely that some parts of the phasic evolution in our study might be different than those reported in the literature because of both different processing methods and the amount of NaF flux. In the current study, the step involving transformation from tetragonal to monoclinic ZrO_2 as reported by Torres *et al.* [17] did not occur given the starting ZrO_2 already being of a monoclinic phase. From the Hedvall effect, it is likely that onset crystallization of SiO_2 at higher than 700°C might trigger the reactions among the starting precursors. This temperature of 700°C was also stated by Pyon *et al.* [15] to induce initiation of zircon crystal formation. As the temperature

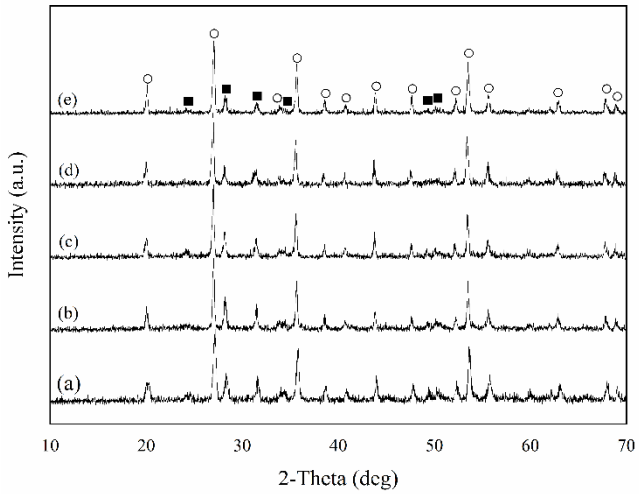

Figure 2. XRD patterns of the pigments from the RHA route fired at 1300°C for 12 h with intermediate grinding. The dopants are (a) undoped, (b) Cr, (c) Fe, (d) Pr, and (e) V. O = $ZrSiO_4$ (Zircon, JCPDS 06-0266), and ■ = monoclinic ZrO_2 (m-ZrO_2, JCPDS 37-1484).

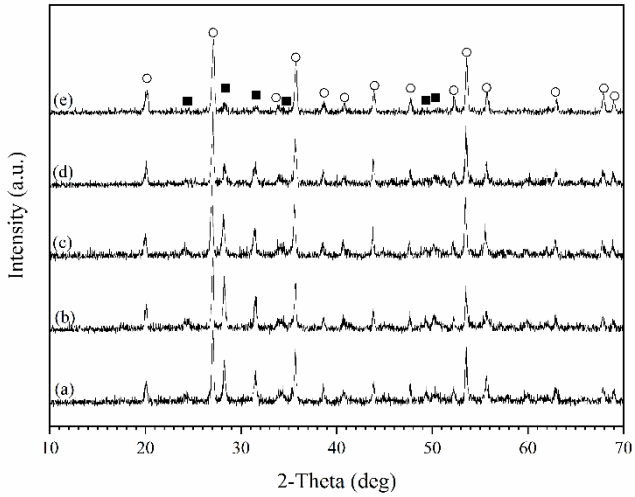

Figure 3. XRD patterns of the pigments from the oxide route (using crystalline SiO_2) fired at 1300°C for 12 h with intermediate grinding. The dopants are (a) undoped, (b) Cr, (c) Fe, (d) Pr, and (e) V. O = $ZrSiO_4$ (Zircon, JCPDS 06-0266), and ■ = monoclinic ZrO_2 (m-ZrO2, JCPDS 37-1484).

Table 1. Phase fractions of the $ZrSiO_4$ and m-ZrO_2 calculated from the tallest peaks of each phase using integrated intensity (peak area) from Lorentzian peak fitting. Both RHA and oxide routes were also compared.

Composition	Phase fraction			
	RHA route		Oxide route	
	$ZrSiO_4$	m-ZrO_2	$ZrSiO_4$	m-ZrO_2
Undoping	0.73	0.27	0.64	0.36
V-doping	0.85	0.15	0.96	0.04
Pr-doping	0.80	0.20	0.74	0.26
Fe-doping	0.71	0.29	0.61	0.39
Cr-doping	0.65	0.35	0.54	0.46

was ramped up, NaF started to melt and act as a facilitator for liquid-phase diffusion of all relevant ions. V_2O_5 itself has a low melting point and could play a major role similar to NaF. We also believe that, given the high degree of openness in the amorphous silica, such reactivity could possibly occur at a lesser level of thermodynamic difficulty. A binary or even ternary system might take place simultaneously. This phenomenon might be able to explain the absence of cristobalite in our study. However, the small m-ZrO_2 peaks could not be eradicate even with long firing of 48 h or higher firing temperature (with intermediate grinding). This m-ZrO_2 was likely from the unreacted precursor as ZrO_2 is highly refractory. In fact, even with sol-gel processing with well-known high chemical homogeneity, no single-phase V-doped zircon has been reported in the literature.

Addition of Pr_6O_{11} was complicated by its nature of various oxidation states. While it is well-known that Pr_6O_{11} is the most common and stable form at normal atmospheric environment, it can be rewritten as $Pr_2O_3.4PrO_2$ which is a mixed oxide with Pr oxidation states of 3+ and 4+ [18]. The Pr:$ZrSiO_4$ pigment was reported to be a substitutional solid solution of Pr^{3+} cation in a zircon crystal structure [11] or Pr^{4+} (0.96 Å) with zircon (Zr^{4+}, 0.84 Å) lattice [4]. However, there were other studies that reported the presence of Pr^{4+} in their samples but with a very small quantity [19,20]. Unfortunately, X-ray Photoelectron Spectroscopy (XPS) in this study could not resolve the peaks corresponding to Pr^{3+} and Pr^{4+} due to resolution inadequacy from a small doping amount. Nevertheless, without the intermediates such as $PrSiO_4$ formed, it is likely that the Pr cations must have been successfully incorporated into the $ZrSiO_4$ structure as reflected by a small enlargement in the cell volume after doping. (261.70 $Å^3$) Trojan [13] was one of the first to propose that the trivalent praseodymium cation must be converted into the tetravalent state (substitution uncharged defects) which could be later incorporated into the zircon structure. Other transitory phases ($Pr_2Zr_2O_7$ and $Na_2Pr_8Si_6O_{24}F_2$) were not found in our study which was in agreement with the report by Blosi *et al.* [21] when using microwave-assisted synthesis. Various studies on Pr-doped $ZrSiO_4$ did not demonstrate the ability to obtain single-phase zircon. The multi-phasic nature of the pigment in our study was in agreement with those studies especially with m-ZrO_2 as a dominant secondary phase [11,14].

Doping with Iron (Fe) could cause the zircon lattice to change due to the difference in the ionic radii among Fe^{3+}, Zr^{4+} and Si^{4+}. Lattice refinement in this study yielded a cell volume after doping to be 260.60 $Å^3$ which was larger than the undoped sample. Hence, it would be probable that the Fe cation choose to replace Si^{4+} instead of Zr^{4+}; the first is smaller than the latter. The similar trend was also reported by Herrera *et al*. [5] whose explanation included the electroneutrality condition. They proposed that, given a lower valence of Fe, oxygen vacancy should be created, resulting in a small enlargement of the cell volume. To the best of our knowledge, no data on lattice parameter change of the Cr-doped zircon has been reported. Our study revealed a slight decrease in the cell volume upon Cr incorporation (260.40 $Å^3$ compared to 260.50 $Å^3$ for the undoped sample). This increase was likely induced by a smaller cationic size of Cr^{3+} (VI, 0.615 Å) relative to Zr^{4+} (VI, 0.72 Å). The substitution of chromium cation in an octahedral lattice site has been a subject of contradictory reports given the chromium itself could possess either 3+ or 4+. A detailed mechanism for this would be subjected to a future study. Nevertheless, alterations in cell volume, along with the color changes, for all four dopant systems suggested successful incorporation of a certain amount of dopants. However, the current results should by no means be interpreted as whether a solid solubility was reached or exceeded.

The particle sizes of the obtained pigments were different in each dopant. Vanadium doping resulted in relatively uniform size distribution in the 2 µm to 5 µm range as shown in Figure 4. The average particle sizes were 3.2, 3.1, 5.0 and 3.3 µm for V, Pr, Fe and Cr dopants, respectively. These values are in relatively similar ranges with several studies [6,16]. In the backscattering mode (BEI), only a small number of particles of lighter contrast (white) was observed; they were likely of ZrO_2 with Zr as a higher atomic number as confirmed by Energy Dispersive Spectroscopy (EDS). The Fe:$ZrSiO_4$ pigments revealed a similar result but with a slightly larger distribution in size. In the BEI mode, three different levels of contrast were observed especially in the abnormal large particles. They are of dark, light grey and white tones, which could be associated distinctive atoms with different atomic numbers. The brightest area represented unreacted zirconia appearing as part of a larger particle as well as in individual particles. Particles with this white tone were observed in all zircon pigment samples; this appearance supports the XRD results showing secondary ZrO_2 peaks in all samples. In addition, elemental analysis was employed to examine the distribution of all four cationic elements in the pigments. Figures 5-8 display mapping of Zr, Si, dopant and O with obtained spectra. All four dopant systems demonstrated common results. The brightest particles revealed a strong level of signal of Zr; the majority of these particles also contained a certain degree of Si.

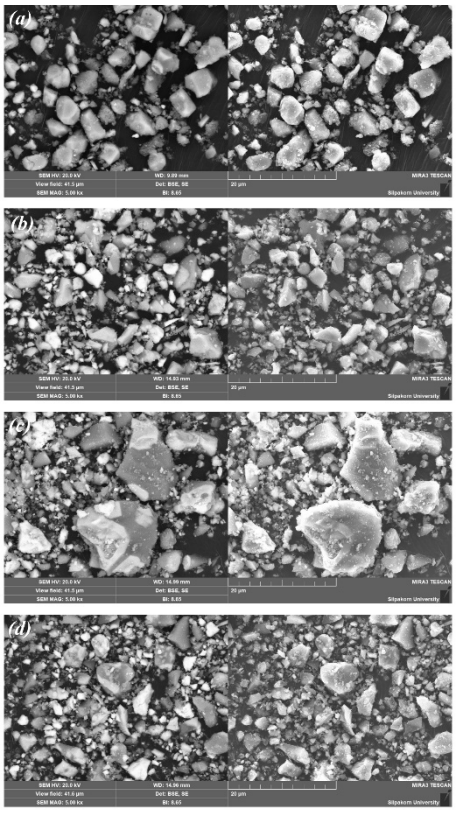

Figure 4. SEM images of the synthesized pigments fired at 1300°C for 12 h. The left side is from the backscattering (BEI) mode whereas the right from the secondary (SEI) mode. The dopants were (a) V, (b) Pr, (c) Fe and (d) Cr.

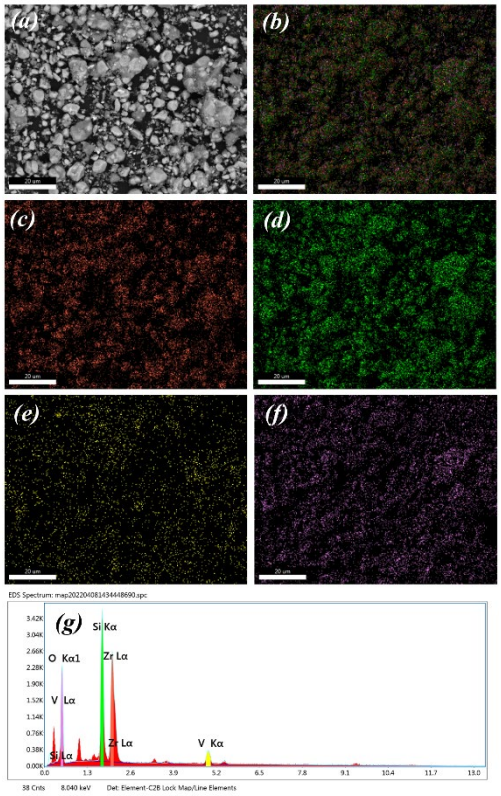

Figure 5. Energy dispersive spectroscopic data of the synthesized V-doped pigments fired at 1300°C for 12 h. The details are (a) Morphology, (b) Overlapping of all elements, (c) Zr, (d) Si, (e) V, (f) O and (g) EDS spectrum.

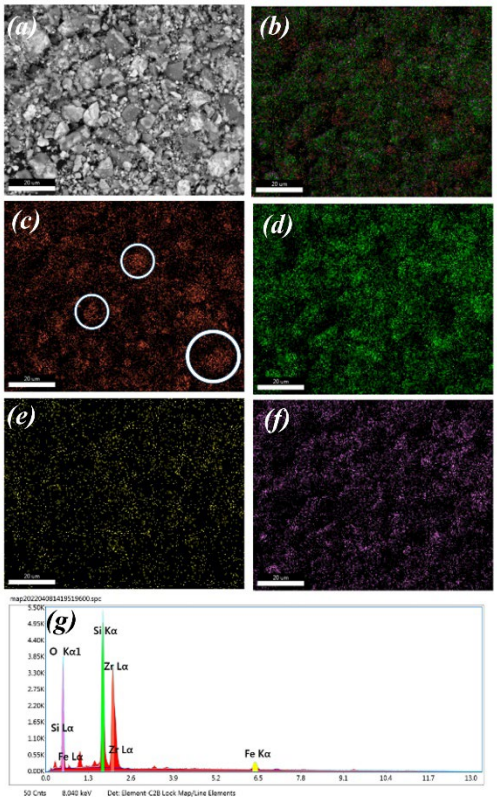

Figure 7. Energy dispersive spectroscopic data of the synthesized Fe-doped pigments fired at 1300°C for 12 h. The details are (a) Morphology, (b) Overlapping of all elements, (c) Zr, (d) Si, (e) Fe, (f) O and (g) EDS spectrum.

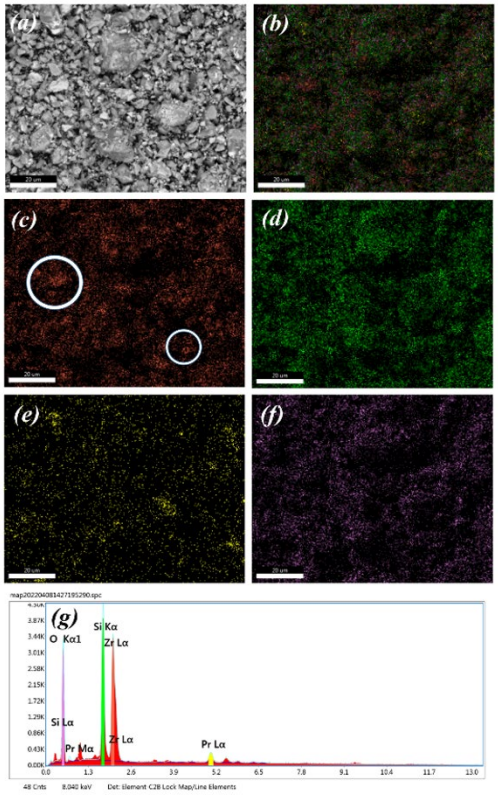

Figure 6. Energy dispersive spectroscopic data of the synthesized Pr-doped pigments fired at 1300°C for 12 h. The details are (a) Morphology, (b) Overlapping of all elements, (c) Zr, (d) Si, (e) Pr, (f) O and (g) EDS spectrum.

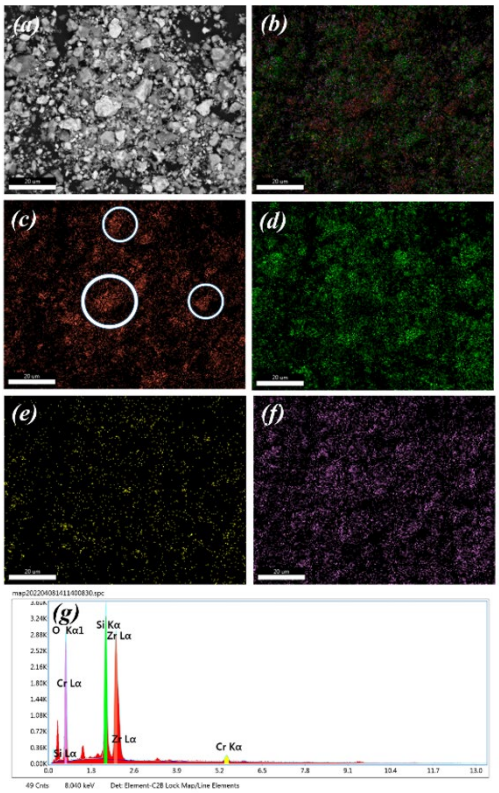

Figure 8. Energy dispersive spectroscopic data of the synthesized Cr-doped pigments fired at 1300°C for 12 h. The details are (a) Morphology, (b) Overlapping of all elements, (c) Zr, (d) Si, (e) Cr, (f) O and (g) EDS spectrum.

There were some particles that contained only Zr and O which could be responsible for the m-ZrO_2 peak detected by XRD. Other particles consisted only Si and O were plausibly amorphous SiO_2 as XRD did not reveal any dominant peak associated with all phases of SiO_2. The dopants (V, Pr, Fe and Cr) were found to almost evenly disperse on the overall particle system. This result could be an indirect indication of solid solution formation as previously reported in the XRD results by the changes in the cell volume by lattice refinement.

The optical properties of the synthesized pigment samples were examined by UV-vis-NIR spectroscopy. Only the visible region (400 nm to 800 nm) was shown in Figure 9 because of visual observation purposes of the pigment. The V-doped zircon sample yielded a broad peak with a maximum of reflectance in the 500 nm range with a highest degree of absorption in the 640 nm range (Figure 9(a)). Ardizzone *et al.* [9] and Pyon *et al.* [15] reported spectra with relatively similarity to what was obtained in this study; the first authors employed a reflectance mode whereas the latter author an absorbance mode. The presence of V^{5+} could be ruled out given the fact that no reflectance peak at approximately 530 nm was observed [9]. The characteristic band at 640 nm was attributed to V^{4+} with tetrahedral and dodecahedral coordination which is the origin of blue color [9,15,16]. This band is caused by the transition from $2B_1$ to 2_E [15]. An increase in reflectance seen as a shoulder at around 750 nm was claimed to be due to a shoulder-forbidden transition of V^{4+} [9].

The yellow tone of the Pr-doped pigment sample was reflected by the characteristic reflectance band in the reflectance spectrum as shown in Figure 9(b). A dominant band could be observed in the 570 nm range, corresponding to the yellow light region (565 nm to 580 nm) [14,22]. Given that the complimentary color of yellow is blue, a minimum of the reflectance spectrum occurred in the 400 nm to 450 nm range; this range was also claimed to be part of characteristic absorption band of yellow [2]. The high intensity (> 80%) of the 570 nm reflectance band in the current study was accompanied by a very high value of the *b* parameter of +49.0 as shown in. The positivity of this b parameter indicates a yellow tone. This value was slightly lower than those reported in the literature [2,14,22] possibly due to the impurity in the RHA as previously explained in the V-doped zircon system. The hue angle of slightly more than 90 suggests coloration of greenish yellow which is accurately reflected by both negative *a* and positive *b* parameters.

Doping with Fe resulted in the UV-vis spectrum (Figure 9(c)) with less dominant bands compared to those of V-doped and Pr-doped samples. Upon a closer consideration, there appeared to be at least three broad bands at 425, 470, 525 and 720 nm. The first two bands were claimed to be from d-d bands associated with tetrahedral Fe^{3+} whereas the others were stated to be attributed to octahedral Fe^{3+} [5]. Similar UV-vis spectra of the Fe-doped $ZrSiO_4$ samples were also reported by K-R. Pyon and B-H. Lee [23]. The green tone of the Cr-doped sample was reflected by a strong reflectance band in the 540 nm range as shown in Figure 9(d). An obvious absorption in the red light region (> 600 nm) was also observed. These results were in agreement with the reports in the literature [6,24]. This reflectance band was likely associated with the d-d transition when Cr cations were incorporated in the Zr lattice site.

Chemical stability of the obtained pigments was preliminarily evaluated with the base glaze and its ingredient compounds by using the Pr-doped pigment as an example. Other frequently used raw materials by artists were also included in the study. The mechanical mixtures between the pigment and base glaze or raw materials were prepared by hand-grinding in a 1:1 weight ratio and later fired at 1200°C for 2 h to mimic the glaze firing condition. The selected weight ratio (1:1) would ensure that sufficient contacts between the pigment and tested raw material particles were achieved. XRD was also carried out for the pigment-containing glaze (10 wt%); however, the XRD peaks of zircon and ZrO_2 were too low to be useful for further assessment. Figure 10 shows the XRD patterns of the fired mixtures with only major secondary phases indexed. The XRD pattern of the synthesized pigment was also included for comparison, and it should be noted that the pigment itself already contained a certain amount of ZrO_2 impurity to begin with.

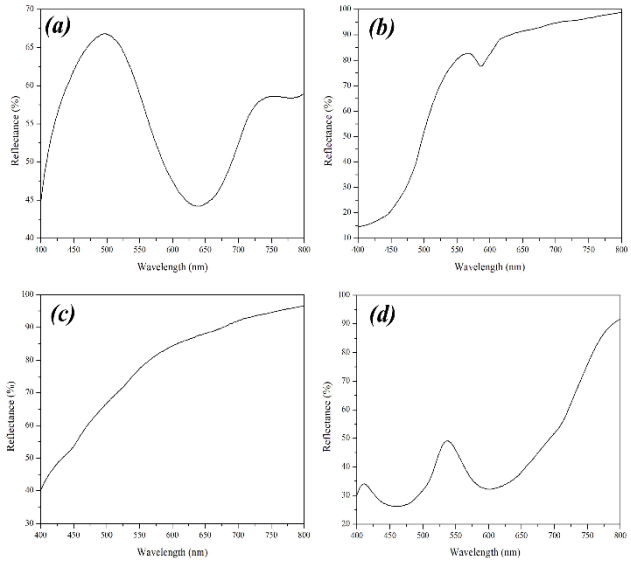

Figure 9. UV-vis spectra of the synthesized pigments fired at 1300°C for 12 hours. (a) V, (b) Pr, (c) Fe and (d) Cr.

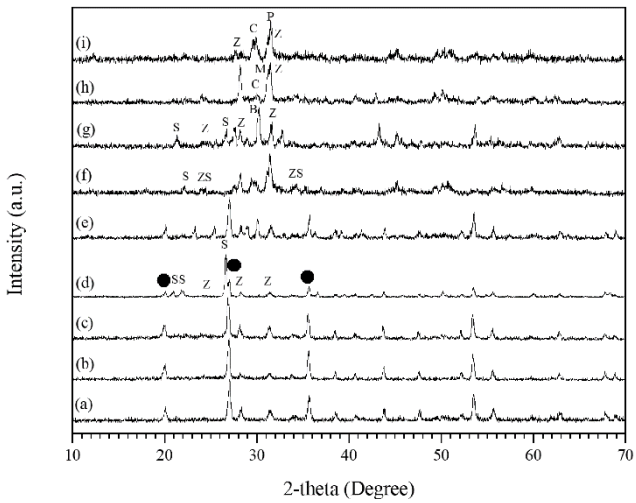

Figure 10. XRD patterns of the mixtures between the pigment and raw materials (1:1 weight ratio) fired at 1200°C for 2 h. The raw materials were (a) Pigment (pure), (b) Base glaze, (c) Na-feldspar, (d) SiO_2, (e) Wollastonite, (f) ZnO, (g) $BaCO_3$, (h) Dolomite and (i) $CaCO_3$. • = $ZrSiO_4$, S = SiO_2, Z = ZrO_2, ZS = Zn_2SiO_4, B = $BaZrO_3$, C = CaO, M = $MgSiO_3$ and P = $CaSiO_3$

Table 2. Color parameters of the glazes with 10 wt% pigments fired at 1200°C for 2 h.

Dopant	Color parameter					Color
	L	***a***	***b***	***C***	***H***	
Vanadium	85.1	-7.0	3.1	7.6	156.0	
Praseodymium	89.0	-7.2	46.3	46.9	98.8	
Chromium	71.6	-1.9	21.7	21.8	85.1	
Iron	88.3	-0.5	13.9	13.9	92.0	

Table 3. Color parameters of the mixtures between tested materials an pigments in the weight ratio of 1:1 fired at 1200°C for 2 hours. The resulting colors reveals how color changes due to instability.

Tested materials	Color parameter					Color
	L	***a***	***b***	***C***	***H***	
$CaCO_3$	81.3	0.1	20.9	20.9	89.7	
Dolomite	91.6	-0.8	15.9	16.0	93.0	
$BaCO_3$	90.3	-1.3	15.3	15.4	94.9	
ZnO	88.1	-1.4	15.7	15.8	95.2	
Wollastonite	93.3	-4.5	25.3	25.7	100.1	
SiO_2	89.6	-5.2	36.5	36.9	98.1	
Na-feldspar	93.7	-6.4	26.3	27.1	103.6	
Base glaze	95.0	-6.9	29.9	30.7	103.0	
Pigment	85.2	-2.1	49.0	49.0	92.4	

Mixing with the base glaze resulted in a significant decrease in the ZrO_2 secondary peak intensity as demonstrated in Figure 10(b). This result was likely caused by the fact that the melted or matured glaze could act as a powerful fluxing agent, enhancing diffusion in a liquid phase and facilitating further reactivity between remaining ZrO_2 with other unreacted SiO_2. The fraction of zircon phase appeared to increase significantly. Na-feldspar ($NaAlSi_3O_8$) did not help improve reactivity as the height of the ZrO_2 peaks was still relatively similar to those of the pigment (Figure 10(c)). The fluxing property of the feldspar in glaze might be expected to facilitate additional reactivity between the unreacted precursors; however, that fluxing role should be considered when being present in a glaze composition only. Another speculation might be related to the fact that zircon has been reported to be decomposed using the alkali fusion method [25]. Nevertheless, Na-feldspar ($NaAlSi_3O_8$) would be much different from NaOH given the fact that, after feldspathic dissociation, Na_2O would not be as basic as that of NaOH. Mixing with SiO_2 seemed to help reduce the intensity of the ZrO_2 peak. However, upon a closer look, the tallest peak in the 27º region was in fact belonged to the SiO_2 quartz phase; the zircon peak at 27º had the intensity of only approximately 40% to that of SiO_2. This proximity between the two phases' peaks, along with visible ZrO_2 peaks, confirmed that mixing with SiO_2 did not help improve phase formation of zircon (Figure 10(d)). Wollastonite ($CaSiO_3$) did not seem to affect the pre-existing zircon and ZrO_2 to a greater extent as shown in Figure 10(e). It has been known that $CaSiO_3$ dissociates into CaO and SiO_2 at high temperatures and behaves in the glaze with the fluxing properties. Detached CaO could react with ZrO_2 to form $CaZrO_3$ as evidenced by a small peak in the 24º region. The sourcing SiO_2 from wollastonite did not seem to form any new compounds; rather, it could be co-existed with the original zircon without any reactivity throughout the reaction time. This claim could be supported by a slightly broad peak in the 27º region which was plausibly composed of both SiO_2 and zircon peaks being in a close proximity to each other. For these three raw materials (Na-feldspar, SiO_2 and wollastonite), the color appearance was still in an obvious yellowish tone as displays in Table 3. The b parameters were still higher than +25 compared to +29.9 of the incorporated base glaze.

On the other hand, ZnO, $BaCO_3$, dolomite ($CaMg(CO_3)_2$) and $CaCO_3$ were demonstrated to have a totally opposite effect. No zircon peaks were visible as shown in Figure 10(f-i). $CaCO_3$ has been reported to cause decomposition of zircon and was proposed as a solution to tackle the cationic incorporation difficulty in the highly stable zircon lattice by first forming an intermediate phase of ZrO_2 [26]. Three major new phases in the $CaCO_3$ system included ZrO_2, CaO and $CaSiO_3$ (perovskite) as displays in Figure 10(i). Quite similar phases also appear when $BaCO_3$ was mixed with the zircon pigment but with more pronounced SiO_2 and newly formed $BaZrO_3$ (Figure 10(g)). $MgSiO_3$ and CaO formed as shown in Figure 9(h) in the dolomite addition case as it readily decomposes in the 800°C range. Similar decomposition of zircon was obvious in the case of dolomite addition. For $BaCO_3$, dolomite ($CaMg(CO_3)_2$) and $CaCO_3$, the cause of such chemical instability could be from the basicity of the alkali earth element (Ca and Ba) during which ZnO seem to react with SiO_2 which was decomposed from the zircon, forming Willemite Zn_2SiO_4 (Figure 10(f)). The role of ZnO in the ability to break up zircon lattice has never been reported in the literature according to the best knowledge of the authors. Nevertheless, it might not be surprising given ZnO itself was known to be a secondary flux. ZnO, $BaCO_3$, dolomite (CaMg

$(CO_3)_2$) and $CaCO_3$, when reacting with the Pr-doped zircon pigments, resulted in the *b* parameter (yellowness) in the 15 to 20 range (Table 3) which were lower than Na-feldspar, SiO_2 and wollastonite. From these XRD patterns and resulting color parameters, this preliminary stability test could offer high potential for tailoring the glaze recipe suitable for the used pigment. It should be noted that the pigments with other types of dopant (V, Fe and Cr) might behave differently and should be tested separately. The detailed investigation of appropriate glaze formulation will be subjected to the future study.

4. Conclusions

Using rice husk ash (RHA) as a substitute for crystalline SiO_2 helped enhance phase formability of zircon in all dopants except vanadium. All samples still contained m-ZrO_2 as a secondary phase. The absence of SiO_2 from XRD suggested that it would likely remain amorphous at the processing temperature. Such enhanced reactivity could be caused by the Hedvall effect. Incorporation of dopant cations was reflected by changes in cell volume likely caused by either differences in ionic size or creation of oxygen vacancy. The particle sizes of the pigments were on average in the 3 μm to 5 μm range which are suitable for practical usage in ceramic glazes. Dopants were found to evenly distribute as examined by mapping elemental analysis. The obtained colors were bluish, yellowish, lightly brownish and greenish for V, Pr, Cr and Fe, respectively. These colorations were confirmed by the CIELab data and UV-vis spectra demonstrating that such colors were contributed from the d-d transition. Retention of color was still maintained when incorporated in a typical feldspathic glaze at its maturation point. Chemical stability tests using the Pr-doped sample revealed that the pigments seemed to be less stable with ZnO, $BaCO_3$, dolomite and $CaCO_3$, all of which have a common characteristic of being highly alkaline with 2+ valence state. Therefore, the synthesized pigments from RHA could be employed as an alternative to their oxide-route pigments. In addition, with the stability data for each common raw material, appropriate formulations of glaze could likely be tailored for Pr-doped zircon in order to retain its yellowness in matured glazes by excluding undesirable raw materials.

Acknowledgements

This research is financially supported by Thailand Science Research and Innovation (TSRI) National Science, Research and Innovation Fund (NSRF) (Fiscal Year 2022)

References

[1] G. Monros, J. Carda, P. Escribano, and J. Alarcon, "Synthesis of V-$ZrSiO_4$ solid solutions," Journal of Materials Science Letters, vol. 9, pp. 184-186, 1990.

[2] K. R. Pyon, and B. H. Lee, "The influence of firing conditions on the color properties of Pr-$ZrSiO_4$ pigments synthesized using rice husk ash," *Journal of the Korean Ceramic Society,* vol. 46, no. 4, pp. 397-404, 2009.

[3] Y. Obukuru, and S. Matsushima, "First-principles energy band calculation of Pr-doped $ZrSiO_4$," *Journal of the Ceramic Society of Japan,* vol. 129, no. 12, pp. 764-769, 2021.

[4] J. A. Badenes, J. B. Vicent, M. Llusar, M. A. Tena, and G. Monros, "The nature of Pr-$ZrSiO_4$ yellow ceramic pigment," *Journal of Materials Science,* vol. 37, no. 7, pp. 1413-1420, 2002.

[5] G. Herrera, N. Montoya, and J. Alarcon, "Synthesis and characterization of iron-doped $ZrSiO_4$ solid solutions from gels," *Journal of American Ceramic Society,* vol. 94, no. 12, pp. 4247-4255, 2011.

[6] Q. Yang, P. Li, and S. Zhang, "Low temperature synthesis of green submicro Cr-$ZrSiO_4$ ceramic pigments by solid-state method," *International Journal of Applied Ceramic Technology,* vol. 18, no. 2, pp. 345-352, 2020.

[7] E. Ozel, and S. Turan, "Production of coloured zircon pigments from zircon," *Journal of the European Ceramics Society,* vol. 27, pp. 1751-1757, 2007.

[8] A. K. Yadav, V. Ponnilavan, and S. Kannan, "Crystallization of $ZrSiO_4$ from a SiO_2−ZrO_2 Binary System: The Concomitant Effects of Heat Treatment Temperature and TiO_2 Additions," *Crystal Growth and Design,* vol. 16, pp. 5493-5500, 2016.

[9] S. Ardizzone, G. Cappelletti, P. Fermo, C. Oliva, M. Scavini, and F. Scime, "Structural and spectroscopic investigations of blue, vanadium-doped $ZrSiO_4$ pigments prepared by a sol−gel route," *Journal of Physical Chemistry,* vol. 109, pp. 22112-22119, 2005.

[10] G. Monros, J. Carda, M. A. Tena, P. Escribano, M. Sales, and J. Alarcon, "Different kinds of solid solutions in the V_2O_5-$ZrSiO_4$-NaF system by sol-gel processes and their characterization," *Journal of the European Ceramic Society,* vol. 11, pp. 77-86, 1993.

[11] J. K. Kar, R. Stevens and C. R. Bowen, "Processing and characterisation of Pr–zircon pigment powder," *Advances in Applied Ceramics,* vol. 104, no. 5, pp. 233-238, 2005.

[12] M. Ocana, A. Caballero, A. R. Gonzalez-Elipe, P. Tartaj, and C. J. Serna, "Valence and localization of praseodymium in Pr-doped zircon," *Journal of Solid State Chemistry,* vol. 139, pp. 412-415, 1998.

[13] M. Trojan, "Synthesis of a yellow zircon pigment," *Dyes and Pigments,* vol. 9, no. 4, pp. 261-273, 1988.

[14] N. Yongvanich, T. Jitpagdee, B. Chukaew, and S. Papathe, "Yellow ceramic pigments from amorphous nanosized oxides using rice husk and zircon," *Proceedings of the 14th Annual IEEE International Conference on Nano/Micro Engineered and Molecular Systems,* pp. 225-228, 2019.

[15] K. R. Pyon, K. S. Han, and B. H. Lee, "Formation and color properties of vanadium doped $ZrSiO_4$ ceramic pigments," *Journal of Ceramic Processing Research,* vol. 12, no. 3, pp. 279-288, 2011.

[16] B. Tanisan, "V-$ZrSiO_4$ ceramic pigments synthesis from m-ZrO_2 and different amorphous silica sources," *Journal of the Australian Ceramic Society,* vol. 57, pp. 1351-1357, 2021.

[17] F. J. Torres, J. V. Folgado, and J. Alarcon, "Structural Evolution and Vanadium Distribution in the Preparation of V^{4+}-$ZrSiO_4$ Solid Solutions from Gels," *Journal of the American Ceramic Society,* vol. 85, no. 4, pp. 794-799, 2002.

[18] I. Aritman, H. Gergeroglu, and N. Sakar, "Comparative study on structural and optical features of undoped and Eu^{3+} doped Pr_6O_{11} synthesized via sol-gel and flame spray pyrolysis," *Open Ceramics,* vol. 5, p. 1000038, 2021.

[19] A. Mekki, K. A. Ziq, D. Holland, and C. F. McConville, "Magnetic properties of praseodymium ions in Na_2O-Pr_2O_3-SiO_2 glasses," *Journal of Magnetism and Magnetic Materials,* vol. 260, pp. 60-69, 2003.

[20] T. P. Gompa, A. Ramanathan, N. T. Rice, and H. S. La Pierre, "The chemical and physical properties of tetravalent lanthanides Pr, Nd, Tb, and Dy," *Dalton Transactions,* vol. 49, pp. 15945-15987, 2020.

[21] M. Blosia, M. Dondi, S. .Albonetti, G. Baldi, A. Barzanti, and C. Zanelli, "Microwave-assisted synthesis of Pr-$ZrSiO_4$, V-$ZrSiO_4$ and Cr-$YAlO_3$ ceramic pigments," *Journal of the European Ceramic Society,* vol. 29, no. 14, pp. 2951-2957, 2009

[22] D. Guo, M. Xie, N. Ma, Q. Yang, Z. Luo, Y. Chu, Y. Zhang, and P. Rao, "Synthesis and characterization of (Pr, Ce)-$ZrSiO_4$ ceramic pigments: The properties of the pigments and the effect of Ce," *Journal of the American Ceramic Society,* vol. 102, no. 5, pp. 2619-2628, 2019

[23] K. R. Pyon, and B. H. Lee, "Effect of iron content and annealing temperature on the color characteristics of Fe-$ZrSiO_4$ coral pink pigments synthesized by Sol-gel method," *Journal of the Ceramic Society of Japan,* vol. 117, no. 3, pp. 258-263, 2009.

[24] P. Li, Q. Yang, and S. Zhang, "Low temperature synthesis and performance investigation of co-doped (Cr, Co)-$ZrSiO_4$ ceramic pigments," *IOP Conf. Series: Materials Science and Engineering,* vol. 677, p. 022086, 2019

[25] A. M. Abdelkader, A. Daher, and E. El-Kashef, "Novel decomposition method for zircon," *Journal of Alloys and Compounds,* vol. 460, no. 1-2, pp. 577-580, 2008

[26] S. R. Reddy, and G. Mandal, "Studies on the Production of Zirconia from Indian Zircon—Part I: $CaCO_3$-$ZrSiO_4$ System," *Transactions of the Indian Ceramic Society,* vol. 33, no. 5-6, pp. 63-69, 1974.